Sensors and Actuators B 149 (2010) 199–204

Contents lists available at ScienceDirect

Sensors and Actuators B: Chemical

journal homepage: www.elsevier.com/locate/snb

Enantiomerically selective vapochromic sensing

Matthew J. Cich[a], Ian M. Hill[a], Aaron D. Lackner[a], Ryan J. Martinez[a], Travis C. Ruthenburg[a], Yuichiro Takeshita[a], Andrew J. Young[a], Steven M. Drew[a,*], Carrie E. Buss[b], Kent R. Mann[b]

[a] Department of Chemistry, Carleton College, Northfield, MN 55057, USA
[b] Department of Chemistry, University of Minnesota, Minneapolis, MN 55455, USA

ARTICLE INFO

Article history:
Received 11 March 2010
Received in revised form 5 May 2010
Accepted 22 May 2010
Available online 31 May 2010

Keywords:
Vapochromic
Chiral
Gas sensor
Platinum double salt materials

ABSTRACT

The double salt materials platinum(II)tetrakis-R-β-methylphenethylisocyanide tetracyanoplatinate(II) (**R-1**) and platinum(II)tetrakis-S-β-methylphenethylisocyanide tetracyanoplatinate(II) (**S-1**) have been synthesized with highly enantiomerically pure isocyanide ligands. The vapochromic behavior of **R-1** and **S-1** has been studied in the presence of a chiral probe vapor to determine if enantiomerically selective sensing is possible with these materials. The wavelength of maximum emission values (λ_{max}) for solid-state vapoluminescence spectra of **R-1** and **S-1** in the presence of enriched R- and S-2-butanol vapor differ by approximately 10 nm while the λ_{max} values for **R-1** and **S-1** under nitrogen are nearly identical. Principal component analysis has been performed on datasets that consist of a series of vapoluminescence spectra of **R-1** and **S-1** as a function of the R/S-2-butanol ratio. Plots of principal component one versus R/S-2-butanol ratio show mirror image trends for **R-1** relative to **S-1**. While care must be taken to control water vapor and monitor **R-1** and **S-1** for possible decomposition, the reported results nevertheless show that **R-1** and **S-1** are capable of enantiomerically selective vapochromic sensing.

1. Introduction

The search for enantiomerically selective materials for sensors [1], heterogeneous asymmetric catalysis [2], and chromatographic media [3] is an active area of research. New materials that could potentially fulfill any of these needs would be welcomed. Chromoatographic techniques are without a doubt the best method for obtaining quantitative information on enantiomeric purity. Nevertheless, sensing materials are useful in that they can provide quick semi-quantitative information on enantiomeric purity at a low cost. Enantiomerically selective sensors based on colorometric techniques [4], solution fluorescence [5], and solid-state fluorescence [6] can be found in the literature. We report here a class of platinum(II) extended linear chain materials with chiral isocyanide ligands that exhibits enantiomeric selectivity for a chiral alcohol through differences in solid-state vapoluminescence.

The vapochromic behavior of platinum(II) extended linear chain materials, particularly platinum(II) double salts, has been well documented in the literature [7,8]. In particular, platinum(II) double salts composed of tetrakisalkylisocyanide platinum(II) dications alternating with tetracyanoplatinate(II) dianions have been shown to have potential application as sensors for a diverse array of organic vapors and humidity [8]. These compounds are characterized by weak platinum–platinum interactions along the stacks of alternating platinum(II) dications and platinum(II) dianions as well as a porous crystalline structure that allows for the reversible facile penetration of volatile organic compounds (VOC's) into the lattice. These VOCs often modify the platinum–platinum interaction, an electronic interaction that makes these materials highly colored and luminescent, leading to observable changes in the solid-state absorption and luminescence spectra. These characteristics make platinum(II) double salts attractive candidates as vapor sensors.

Herein we report the synthesis and characterization of two platinum(II) double salt materials composed of enantiomerically pure chiral isocyanides: platinum(II) tetrakis-R-β-methylphenethylisocyanide tetracyanoplatinate(II) (**R-1**) and platinum(II) tetrakis-S-β-methylphenethylisocyanide tetracyanoplatinate(II) (**S-1**). The ability of these solid-state materials to differentiate between R- and S-2-butanol has been used as a test case to determine if enantiomerically selective vapochromic sensing is possible. Analysis of sets of solid-state vapoluminescence spectra demonstrates that this pair of materials does detect mixtures of R- and S-2-butanol in a differential manner indicative of enantiomeric selectivity.

2. Experimental

2.1. Synthetic methods

During the course of this study it was determined that high enantiomeric purity of the R- and S-β-methylphenethylamine starting materials was critical to making double salts that were

* Corresponding author. Tel.: +1 507 222 4032; fax: +1 507 222 4400.
E-mail address: sdrew@carleton.edu (S.M. Drew).

0925-4005/$ – see front matter © 2010 Elsevier B.V. All rights reserved.
doi:10.1016/j.snb.2010.05.059

stable and demonstrated enantiomerically selective vapochromic sensing. Chiral HPLC analysis (Chiral Technologies Chiralcel OD–RH 250 × 4.6 mm column, 25:75 acetonitrile:0.1 M KPF_6, pH 2) was used to determine that Fluka was the best source for R- and S-β-methylphenethylamine (both were found to be >99% one enantiomer). The enantiomeric purity of the isocyanide ligands in the final double salt materials **R-1** and **S-1** was assumed to be the same as the amine starting materials. Phosphorous oxychloride (ReagentPlus) and anhydrous acetonitrile were purchased from Aldrich. Dichloromethane and triethylamine were purified by distillation before use. Toluene and 88% formic acid were reagent grade.

FTIR spectroscopy of solids were carried out using the attenuated total reflectance (ATR) method on a ZnSe ATR crystal. Visible spectra of solid double salt materials were obtained using an in-house constructed visible ATR spectrophotometer based on a cubic zirconium ATR crystal. Thin films of formamide and isocyanide products were cast from dichloromethane solution while thin films of double salt materials were formed from a suspension of fine crystallites in diethylether. Combustion analysis was performed by Galbraith Laboratories.

2.1.1. β-Methylphenethylformamide

Typically 1.0 g (7.4 mmol) of β-methylphenethylamine (Fluka) and 4.5 mL of 88% formic acid were dissolved in 50 mL of toluene. This solution was brought to reflux on a Dean-Stark apparatus. The solution collected in the Dean-Stark apparatus was recycled back into the boiling flask several times over a 2-h period after which the solution was refluxed for an additional 16–20 h. Rotary evaporation of the remaining toluene afforded an oily product that was put under vacuum overnight. Yields tended to be nearly quantitative. R-β-methylphenethylformamide: ^{1}H NMR (400 MHz, $CDCl_3$): δ 1.30 (d, 3H, CH_3), 2.95 (m, 1H, CH), 3.28, 3.72 (E/Z rotamer, m, 2H, CH_2), 5.40 (broad, 1H, NH), 7.20 (m, 5H, C_6H_5), 7.80, 8.05 (E/Z rotamer, s, 1H, CHO). FTIR (ATR, ZnSe crystal): $\nu_{C=O}$ 1658 cm^{-1} (s). S-β-methylphenethylformamide: ^{1}H NMR (400 MHz, $CDCl_3$): δ 1.30 (d, 3H, CH_3), 2.95 (m, 1H, CH), 3.28, 3.72 (E/Z rotamer, m, 2H, CH_2), 5.40 (broad, 1H, NH), 7.20 (m, 5H, C_6H_5), 7.80, 8.05 (E/Z rotamer, s, 1H, CHO). FTIR (ATR, ZnSe crystal): $\nu_{C=O}$ 1653 cm^{-1} (s).

2.1.2. β-Methylphenethylisocyanide

Isocyanides were synthesized using the method of Ugi and Meyr [9]. Typically 1.2 g (7.4 mmol) of formamide and 9.7 mL of distilled triethylamine (TEA) were dissolved in 20 mL of distilled dichloromethane. The solution was stirred at 0 °C under argon and a mixture of 1.4 mL phosphorus oxychloride and 2 mL dichloromethane was added dropwise over a 10 min period. The solution was stirred for an additional hour at 0 °C. IR spectra were taken in order to monitor the progress of the reaction. The disappearance of the formamide C=O stretch and the appearance of the C≡N stretch indicated completion of the reaction. The reaction was carefully quenched with 30 mL of an aqueous buffer solution containing 100 mM NaCl and 100 mM sodium dihydrogenphosphate (pH = 7). The organic layer was then washed five times with 30 mL portions of buffer solution. Thorough washes were necessary in order to prevent TEA contamination in the product. The final organic layer was dried overnight in a refrigerator over $MgSO_4$. The solution was filtered and the remaining dichloromethane was removed by rotary evaporation to give an odiferous brown oil. Typical yield was 65–70%. Due to the propensity of β-methylphenethylisocyanide to polymerize it was used immediately. R-β-methylphenethylisocyanide: ^{1}H NMR (400 MHz, $CDCl_3$): δ 1.41 (d, J = 6.96 Hz, 3H, CH_3), 3.10 (sextet, J = 6.84 Hz, 1H, CH), 3.51 (ddq, J = 14.65, 6.78, 1.83 Hz, 2H, CH_2), 7.28 (m, 5H, C_6H_5). FTIR (ATR, ZnSe crystal): $\nu_{C\equiv N}$ 2147 cm^{-1} (s). S-β-methylphenethylisocyanide: ^{1}H NMR (400 MHz, $CDCl_3$): δ 1.41 (d, J = 6.96 Hz, 3H, CH_3), 3.09 (sextet, J = 7.14 Hz, 1H, CH), 3.50 (ddq, J = 14.65, 6.87, 1.77 Hz, 2H, CH_2), 7.27 (m, 5H, C_6H_5). FTIR (ATR, ZnSe crystal): $\nu_{C\equiv N}$ 2147 cm^{-1} (s).

2.1.3. Platinum(II)tetrakis-β-methylphenethylisocyanide tetracyanoplatinate(II)

Platinum(II)tetrakis-acetonitrile triflate ($[Pt(II)(CH_3CN)_4](trif)_2$) and tetrabutylammonium tetracyanoplatinate ($(TBA)_2[Pt(II)(CN)_4]$) were synthesized by literature methods [10–12]. β-methylphenethylisocyanide was used immediately after it was synthesized to minimize problems with isocyanide decomposition. The following procedure was followed: 0.17 g (0.25 mmol) of $[Pt(II)(CH_3CN)_4](trif)_2$ and 1.0 mmol of β-methylphenethylisocyanide were dissolved in 8.0 mL of dry acetonitrile. The solution was stirred at 0 °C under argon for 20 min. ATR–FTIR spectra was taken in order to confirm the formation of the platinum(II)tetrakis-β-methylphenethylisocyanide dication via the expected shift in the C≡N stretch. Next, 0.20 g (0.25 mmol) of $(TBA)_2[Pt(II)(CN)_4]$ dissolved in minimum amount of dry acetonitrile (typically around 5 mL) was added dropwise at 0 °C. The solution was stirred at 0 °C for an additional hour then stored at −20 °C overnight. By the next day a bright red solid was present at the bottom of the flask. The product was collected by filtration and washed with cold, dry acetonitrile and diethylether. The product had a slight solubility in dichloromethane, however, decomposition was rapid precluding the acquisition of NMR spectra. Platinum(II)tetrakis-R-β-methylphenethylisocyanide tetracyanoplatinate(II) (**R-1**): FTIR (ATR, ZnSe crystal): $\nu_{C\equiv NR}$ 2278 cm^{-1} (s); $\nu_{C\equiv N}$ 2124 cm^{-1} (m). Visible spectrum (ATR, cubic zirconia crystal, N_2): λ_{max} = 495 nm. Solid-state luminescence (λ_{ex} = 405 nm, N_2): λ_{max} = 689 nm. Melting point: 69 °C (dec. to yellow solid). Anal. Calcd for $C_{44}H_{44}N_8Pt_2 \cdot H_2O$: C, 48.35; H, 4.24; N, 10.25. Found: C, 48.13; H, 4.41; N, 10.13. Platinum(II)tetrakis-S-β-methylphenethylisocyanide tetracyanoplatinate(II) (**S-1**): FTIR (ATR, ZnSe crystal): $\nu_{C\equiv NR}$ 2276 cm^{-1} (s); $\nu_{C\equiv N}$ 2125 cm^{-1} (m). Visible spectrum (ATR, cubic zirconia crystal, N_2): λ_{max} = 495 nm. Solid-state luminescence (λ_{ex} = 405 nm, N_2): λ_{max} = 692 nm. Melting point: 69 °C (dec. to yellow solid). Anal. Calcd for $C_{44}H_{44}N_8Pt_2 \cdot 2H_2O$: C, 47.56; H, 4.35; N, 10.09. Found: C, 47.88; H, 4.23; N, 10.14.

2.2. Two channel solid-state vapoluminescence measurements

Vapoluminescence measurements were made with an in-house constructed two channel excitation/emission gas flow apparatus. A schematic diagram of this solid-state vapoluminescence apparatus is shown in Fig. 1. The excitation source consisted of two light emitting diodes (LED λ_{ex} = 400 nm, RL5-UV1215, SuperBrightLEDs.com). The light from the LEDs was switched on and off through a pair of transistors on an LED controller circuit board that was interfaced to a multifunction data acquisition (DAQ) board on a computer workstation. The light from each LED was first passed through a band pass filter (Semrock Brightline, FF01-395/11-25) before each entered a separate bifurcated fiber optic excitation/emission probe (CeramOptec, R400-7-2.0M-UV/VIS). Each fiber optic probe guided excitation light into a separate flow cell (brass Swagelok cross with 0.25 in. compression fittings) each with a double salt sample platform, one that held a solid thin film sample of **R-1** (Channel One) and one that held a solid thin film sample of **S-1** (Channel Two). Sample platforms were constructed from 0.25 in. dia. black Delrin pegs. Thin film samples of **R-1** and **S-1** were prepared by drip casting from diethylether suspensions onto the ends of the Delrin pegs. Nitrogen gas was used to move R/S-2-butanol (Aldrich) saturated vapor through the flow cell. Saturated vapor was generated by slowing bubbling N_2 through R/S-2-butanol at room temperature (about 22 °C). The vapor exited the flow apparatus

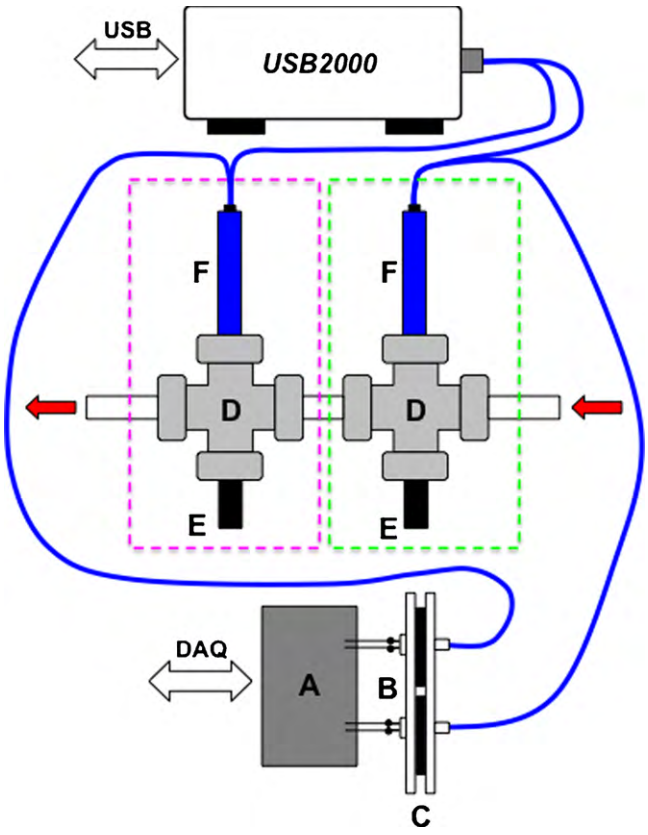

Fig. 1. Two channel solid-state vapoluminescence apparatus. (A). LED controller circuit board. (B). 400 nm LED's. (C). LED and band pass filter holder. (D). Flow cell. (E). Double salt sample platform. F. Bifurcated fiber optic excitation/emission probe. Red arrows indicate direction of nitrogen/vapor flow. Green dashed box: Channel One containing **R-1**. Pink dashed box: Channel Two containing **S-1**. (For interpretation of the references to color in this figure legend, the reader is referred to the web version of the article.)

through an oil bubbler. Nitrogen gas flow was kept at a minimum to ensure that R/S-2-butanol partial pressure in the flow cell was close to its vapor pressure (4.9 Torr @ 22 °C) [13]. Vapoluminescence from solid thin film samples of **R-1** and **S-1** on each Delrin peg was collected by separate bifurcated fiber optic excitation/emission probes. The emission from the two probes entered another bifurcated fiber optic (CeramOptec, UV600/660/2.0 M) that guided the emitted light into a spectrometer (Ocean Optics USB2000). Note that just one spectrometer was needed because only the excitation LED on Channel One or Channel Two was illuminated at any given time. A custom LabVIEW VI (National Instruments) was written to coordinate the timing of excitation LED illumination on a specific channel of the vapoluminescence apparatus with the spectral data acquisition at the spectrometer.

Through the course of a series of experiments it was determined that differences in residual water between **R-1** and **S-1** were affecting the observed vapoluminescence spectra. These differences could be minimized by casting the films from suspensions in "wet" diethylether (saturated with water). A typical vapoluminescence dataset was acquired using the following procedure. Before exposure to R/S-2-butanol vapor, films of **R-1** and **S-1** were exposed to either dry nitrogen or nitrogen saturated with acetonitrile vapor. Typical equilibration times were 10 min. R/S-2-butanol exposures followed and were also equilibrated for 10 min before vapoluminescent spectra were recorded. R/S-2-butanol ratios were determined by chiral capillary GC (Astec Chiraldex beta-bonded B-PM 30 m × 0.25 mm) of the liquid mixtures used to generate vapor. Random samples of R/S-2-butanol were selected between N_2/acetonitrile exposures until all the R/S-2-butanol samples had been used, then the random selection process started again for the next set of replicate exposures.

2.3. Principal component analysis

The analysis of patterns present in sets of solid-state vapoluminescence spectra was aided by Principal Component Analysis (PCA) [14,15]. In preparation for PCA the spectra were first preprocessed by mean centering. PCA of the mean-centered dataset was performed using a custom program written in LabVIEW. For all the data analyzed by PCA in this study 99% of the variance could be accounted for with two principal components.

3. Results and discussion

R-1 and **S-1** were obtained as bright red luminescent solids with one or two adsorbed water molecules, respectively. While we were unsuccessful at obtaining X-ray quality crystals of **R-1** and **S-1**, double salts of this general type have been previously reported [7,8] and some have been structurally characterized by X-ray crystallography [7d]. Based on similarities in color and composition, it is very likely that **R-1** and **S-1** have a structure similar to the representation shown in Scheme 1 where platinum–platinum interactions and vapor channels are present. The proximity of the chiral centers of the isocyanide ligands to the platinum–platinum interaction axis suggests that enantiomeric vapor sensing might be possible

Solid-state vapoluminescence spectra were simultaneously recorded for **R-1** and **S-1** as known mixtures of R/S-2-butanol vapor were carried by a nitrogen stream through the two channel vapoluminescence flow cell. The vapoluminescent response of **R-1** and **S-1** to R/S-2-butanol was used to probe for the presence of enantiomeric selectivity in these double salt materials. Note that the enantiomeric purity of commercially available R-2-butanol was determined to be 91/9 R/S while S-2-butanol was determined to be 10/90 R/S by chiral capillary column GC. Some representative vapo-

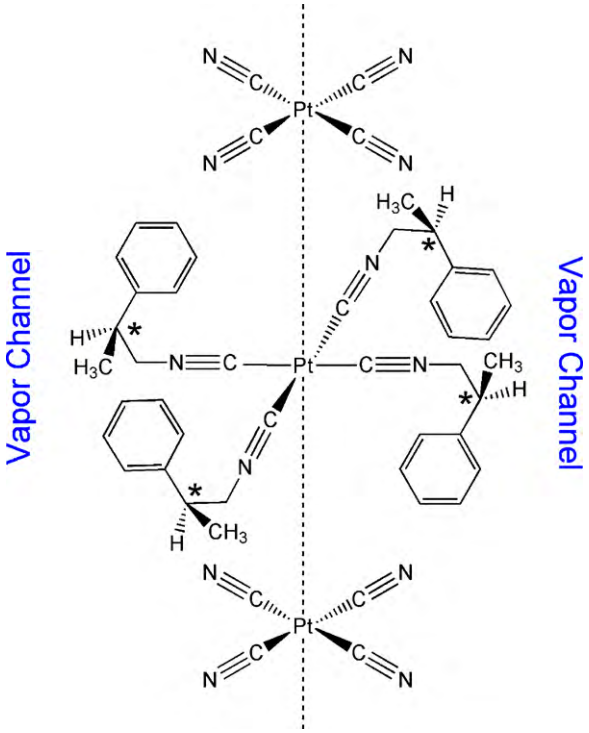

Scheme 1. Schematic representation of **S-1** showing 1.5 units of the proposed double salt structure. Platinum–platinum interactions are indicated by the dotted line. Each isocyanide chiral center is indicated with an asterisk.

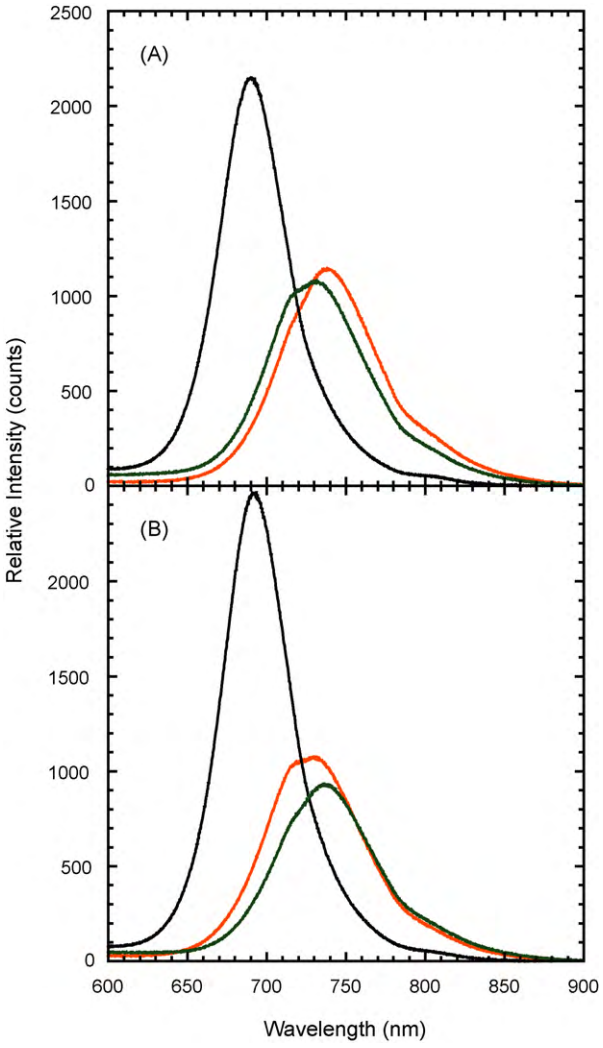

Fig. 2. Solid-state vapoluminescence spectra. A. **R-1**; B. **S-1**. Nitrogen (black), 10/90 R/S-2-butanol (green), 91/9 R/S-2-butanol (orange). (For interpretation of the references to color in this figure legend, the reader is referred to the web version of the article.) (For interpretation of the references to color in this figure legend, the reader is referred to the web version of the article.)

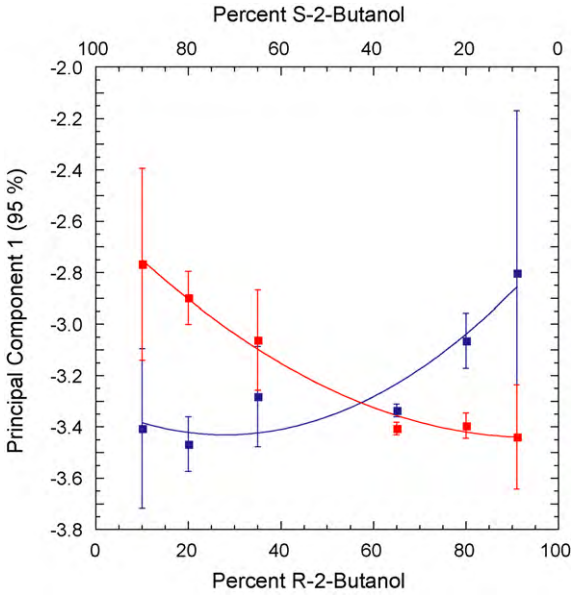

Fig. 3. Principal component 1 versus percent R/S-2-butanol for vapoluminescence of **R-1** (red) and **S-1** (blue). Solid line fits are second order polynomials. Error bars are one standard deviation. (For interpretation of the references to color in this figure legend, the reader is referred to the web version of the article.) (For interpretation of the references to color in this figure legend, the reader is referred to the web version of the article.)

luminescence spectra are shown in Fig. 2. The replicate nitrogen exposures elicited very similar solid-state luminescence spectra for **R-1** and **S-1** with wavelength of maximum emission (λ_{max}) values of 689 and 692 nm, respectively. The small differences in λ_{max} could be caused by slight differences in the absorbed water content or the optical purity of **R-1** versus **S-1**. Exposure of **R-1** and **S-1** to enantiomerically enriched R/S-2-butanol led to much more significant differences in the observed spectra. As seen in Fig. 2A λ_{max} for the solid-state luminescence spectrum of **R-1** in the presence of 91/9 R/S-2-butanol (739 nm) was at longer wavelength than the corresponding spectrum under 10/90 R/S-2-butanol (729 nm). For **S-1** this order was reversed (see Fig. 2B). The solid-state vapoluminescence spectrum of **S-1** in the presence of 10/90 R/S-2-butanol gave a λ_{max} of 737 nm that was at longer wavelength than the corresponding spectrum under 91/9 R/S-2-butanol where λ_{max} is 726 nm. This inverted behavior suggests enantiomeric differentiation is occurring in the vapoluminescent spectra of **R-1** and **S-1**.

To further characterize the vapoluminescent response of **R-1** and **S-1** these materials were exposed to varying ratios of R/S-2-butanol vapor. Vapoluminescent spectra of **R-1** and **S-1** were acquired in the presence of 91/9, 80/20, 65/35, 35/60, 20/80, and 10/90 R/S-2-butanol then analyzed by PCA. As seen in Fig. 3 a plot of principal component 1 (PC1) versus the R/S-2-butanol ratio revealed the expected behavior for enantiomerically selective vapoluminescence. As the percent of R-2-butanol vapor increased, PC1 for one enantiomer increased (**S-1**) while PC1 for the other (**R-1**) decreased. Qualitative examination of the data indicated a gentle curvature to the trend. Therefore, a second order polynomial was fit to the data, not as a physical model, but to highlight the observed trend. Line fits to the data cross near 50/50 R/S-2-butanol and are approximate mirror images of each other. For the case of 10/90 R/S-2-butanol exposure, the difference in the **R-1** versus **S-1** vapoluminescent response is great enough to differentiate the two spectra at the 90% confidence level. However, due to scatter in the data it is not possible to differentiate the vapoluminescent response of **R-1** and **S-1** to 91/9 R/S-2-butanol at the same confidence level. Interestingly, as the R/S-2-butanol ratio approaches racemic it generally becomes easier to differentiate the response of **R-1** from **S-1** until the same response is obtained for racemic R/S-2-butanol.

While the observed vapoluminescence spectral trends for **R-1** and **S-1** in the presence of R/S-2-butanol vapor are not sufficient to delineate the precise mechanism for enantiomeric selectivity, there are several mechanisms that could be possible. For example, differential solvation could be occurring at the chiral sites near the Pt–Pt chromophore when R/S-2-butanol vapor is present. If R-2-butanol intermolecular interactions with the chiral centers of **R-1** have a different degree of energetic favorability relative to the intermolecular interactions of S-2-butanol at the chiral centers of **R-1**, this will manifest itself in a shift of the vapoluminescence spectrum of **R-1** relative to **S-1** following a mirror image trend. As an alternative explanation, differential selective hydrogen bonding between the R/S-2-butanol and the cyanide ligands [7c] in **R-1** and **S-1** could result from the introduction of the chiral sites on the alkylisocyanide ligands. This mechanism will also have an effect of the electronic state of the Pt–Pt chromophore and, therefore, the observed vapoluminescence spectra. Another possible mechanism is that the presence of the chiral centers on **R-1** and **S-1** could lead to selective permeation of R/S-2-butanol into the interstitial voids of **R-1** and **S-1**. This would alter the ratio of R/S-2-butanol in **R-1** and

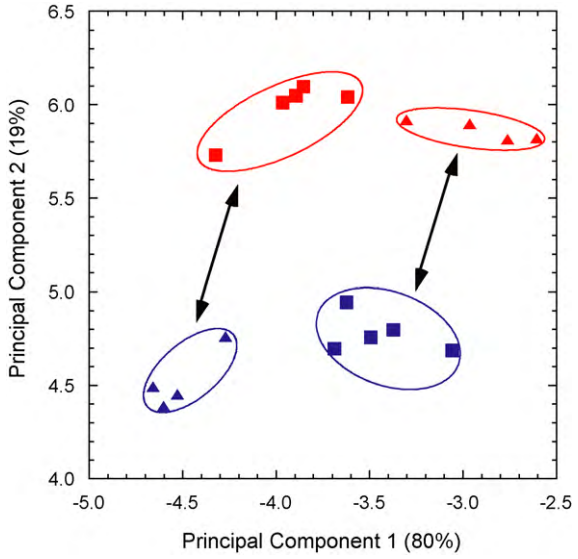

Fig. 4. The effect of differential absorbed water in **R-1** (red) and **S-1** (blue). 91/9 R/S-2-butanol (triangles) and 10/90 R/S-2-butanol (squares). Clusters of data are enclosed in ellipses for clarity. Arrows indicate clusters that merge when differences in absorbed water are minimized. (For interpretation of the references to color in this figure legend, the reader is referred to the web version of the article.) (For interpretation of the references to color in this figure legend, the reader is referred to the web version of the article.)

S-1 relative to the ratio found in the gas phase. Because the sensing mechanism is a convolution of permeation into the double salt material and molecular interaction between the double salt material and the chiral vapor, it is very difficult to separate these two processes. It is very likely the observed vapoluminescence spectral trends are caused by a combination of these three effects.

The vapoluminescence spectra of **R-1** and **S-1** were found to be significantly affected by water vapor. Therefore, care was taken to either minimize the presence of water vapor or ensure that water vapor content remained constant. Unfortunately, the problem of differences in absorbed water content in thin films of **R-1** and **S-1** could not be dealt with by flash heating of the double salts [8b,c] because of the relatively low melting point of these materials (69 °C). Instead, differences in absorbed water in **R-1** and **S-1** were equalized by drip casting films from "wet" diethylether. Failure to follow this procedure led to vapoluminescence spectra that were offset in PC1 and required two principal components to capture most of the variance in the dataset. For example, Fig. 4 shows the results of an experiment where no effort was made to equalize the absorbed water content in **R-1** and **S-1**. In this case **R-1** and **S-1** thin films were prepared by drip casting from "dry" diethylether. Replicate exposures of **R-1** and **S-1** prepared in this manner to 10/90-R/S-2-butanol and 91/9-R/S-2-butanol are shown in Fig. 4. In this case the spectra for **R-1** exposed to 10/90-R/S-2-butanol did not align along PC1 with the spectra for **S-1** exposed to 91/9-R/S-2-butanol (compare the red squares to the blue triangles) and there is a significant amount of variance found in a second principal component (PC1: 80%, PC2: 19%). However, when "wet" diethylether was used to form the films, the spectra for **R-1** exposed to 10/90-R/S-2-butanol aligned along PC1 with the spectra for **S-1** exposed to 91/9-R/S-2-butanol (see Fig. 3). In addition, 95% of the variance in these spectra was represented in PC1 and the variance represented by PC2 was substantially reduced (PC2: 4%). Presumably, PCA was not able to completely isolate the effects of absorbed water differences into only one principal component. However, the fact that PC2 could be minimized significantly by using the appropriate film casting method implies that its presence is a good indicator of differences in absorbed water between **R-1** and **S-1**.

Films of **R-1** and **S-1** were observed to have a limited lifetime in the vapoluminescence flow apparatus. After about 40–50 exposures to 2-butanol vapor the vapoluminescence spectra began to shift to a lesser degree than observed in the earlier exposures. If exposed to solvent vapor continuously for a day at room temperature **R-1** and **S-1** decomposed to a yellow product similar in color to the product observed when **R-1** and **S-1** were melted at 69 °C. This yellow product was likely the more thermodynamically stable isomeric "neutral" that would be formulated as cis-Pt(II)(β-methylphenethylisocyanide)$_2$(CN)$_2$ [16].

4. Conclusion

We have obtained evidence that suggests enantiomerically selective vapoluminescent sensing is possible with chiral platinum(II) double salt materials. While this particular example is fraught with problems related to the interference of water vapor and limited stability, the data nevertheless show that **R-1** and **S-1** materials are enatiomerically selective under carefully controlled conditions. Research is ongoing into the enantiomeric selectivity of other double salt materials composed of chiral isocyanides to determine if the water sensitivity and stability issues observed with **R-1** and **S-1** can be overcome.

Acknowledgements

We are thankful for the support of the NSF RSEC grant administered by the University of Minnesota. In addition S.M.D. would like to recognize the Donors of the American Chemical Society Petroleum Research Fund for support of this research in addition to the support of Carleton College's Howard Hughes Medical Institute grant. Work in the laboratory of K.R.M. was supported by the Center for Process Analytical Chemistry and the Initiative for Renewable Energy and the Environment.

References

[1] (a) M. Trojanowicz, M. Kaniewska, Electrochemical chiral sensors and biosensors, Electroanalysis 21 (2009) 229–238;
(b) G.A. Hembury, V.V. Borovkov, Y. Inoue, Chirality-sensing supramolecular systems, Chem. Rev. 108 (2008) 1–73;
(c) C.-J. Lee, J. Yang, α-Cyclodextrin-modified infrared sensing system for rapidly determining the enantiomeric composition of chiral compounds, Talanta 74 (2008) 1104–1112;
(d) L. Torsi, G.M. Farinola, F. Marinelli, M.C. Tanese, O.H. Omar, L. Valli, F. Babudri, F. Palmisano, P.G. Zambonin, F. Naso, A sensitivity-enhanced field-effect chiral sensor, Nat. Mater. 7 (2008) 412–417;
(e) D. Nopper, O. Lammershop, G. Wulff, G. Gauglitz, Amidine-based molecularly imprinted polymers–new sensitive elements for chiral chemosensors, Anal. Bioanal. Chem. 377 (2003) 608–613;
(f) M. Wehner, T. Schrader, P. Finocchiaro, S. Failla, G. Consiglio, A chiral sensor for arginine and lysine, Org. Lett. 2 (1999) 605–608;
(g) O. Hofstetter, H. Hofstetter, M. Wilchek, V. Schurig, B.S. Green, Chiral discrimination using an immunosensor, Nat. Biotech. 17 (1999) 371–374.
[2] (a) K. Ding, Y. Uozumi, Handbook of Asymmetric Heterogeneous Catalysis, Wiley-VCH, Weinheim, Germany, 2008;
(b) J.M. Thomas, R. Raja, Exploiting nanospace for asymmetric catalysis: confinement of immobilized, single-site chiral catalysts enhances enantioselectivity, Acc.Chem. Res. 41 (2007) 708–720.
[3] G. Subramanian, Chiral Separation Techniques: A Practical Approach, third ed., Wiley-VCH, Weinheim, Germany, 2007.
[4] (a) Z.H. Chen, Y.B. He, C.G. Hu, X.H. Huang, L. Hu, Synthesis and chiral recognition properties of a novel colorimetric chiral sensor for carboxylic anions, Aust. J. Chem. 61 (2008) 310–315;
(b) K. Tsubaki, M. Nuruzzaman, T. Kusumoto, N. Hayashi, W. Bin-Gui, K. Fuji, Visual enantiomeric recognition using chiral phenolphthalein derivatives, Org. Lett. 3 (2001) 4071–4073;
(c) Y. Kubo, S. Maeda, S. Tokita, M. Kubo, Colorimetric chiral recognition by a molecular sensor, Nature 382 (1996) 522–524;
(d) F. Vogtle, P. Knops, Dyes for visual distinction between enantiomers: crown ethers as optical sensors for chiral compounds, Angew. Chem. Int. Ed. 30 (1991) 958–960;
(e) T. Kaneda, K. Hirose, Misumi S S., Chiral azophenolic acerands: color indicators to judge the absolute configuration of chiral amines, J. Am. Chem. Soc. 111 (1989) 742–743.

[5] (a) L. Chi, J. Zhao, T.D. James, Chiral mono boronic acid as fluorescent enantioselective sensor for mono α-hydroxyl carboxylic acids, J. Org. Chem. 73 (2008) 4684–4687;
(b) S.P. Upadhyay, R.R.S. Pissurlenkar, E.C. Coutinho, A.V. Karnik, Furo-fused BINOL based crown as a fluorescent chiral sensor for enantioselective recognition of phenylethylamine and ethyl ester of valine, J. Org. Chem. 72 (2007) 5709–5714;
(c) L. Pu, Fluorescence of organic molecules in chiral recognition, Chem. Rev. 104 (2004) 1687–1716;
(d) K.H. Ahn, H. Ku, Y. Kim, S.G. Kim, Y.K. Kim, H.S. Son, J.K. Ku, Fluorescence sensing of ammonium and organoammonium ions with tripodal oxazoline receptors, Org. Lett. 5 (2003) 1419–1422.
[6] H.L. Liu, X.L. Hou, L. Pu, Enantioselective precipitation and solid-state fluorescence enhancement in the recognition of α-hydroxycarboxylic acids, Angew. Chem. Int. Ed. 48 (2009) 382–385.
[7] (a) C.L. Exstrom, J.R. Sowa, C.A. Daws, D.E. Janzen, G.A. Moore, F.F. Stewart, K.R. Mann, Inclusion of organic vapors by crystalline, solvatochromic $[Pt(aryl\ isonitrile)_4][Pd((CN)_4]$ compounds 'Vapochromic' environmental sensors, Chem. Mater. 7 (1995) 15–17;
(b) C.A. Daws, C.L. Exstrom, J.R. Sowa, K.R. Mann, Vapochromic compounds as environmental sensors. 2. Synthesis and near-infrared and infrared spectroscopy studies of $[Pt(arylisocyanide)_4][Pt(CN)_4]$ upon exposure to volatile organic compound vapors, Chem. Mater. 9 (1997) 363–368;
(c) C.L. Exstrom, M.K. Pomije, K.R. Mann, Infrared spectroscopy studies of platinum salts containing tetracyanoplatinate(II). Evidence for strong hydrogen-bonding interactions in 'vapochromic' environmental sensor materials, Chem. Mater. 10 (1998) 942–945;
(d) C.E. Buss, C.E. Anderson, M.K. Pomije, C.M. Lutz, D. Britton, K.R. Mann, Structural investigations of vapochromic behavior. X-ray single-crystal and powder diffraction studies of $[Pt(CN\text{-}iso\text{-}C_3H_7)_4][M(CN)_4]$ for M = Pt or Pd, J. Am. Chem. Soc. 120 (1998) 7783–7790.
[8] (a) S.M. Drew, D.E. Janzen, C.E. Buss, D.I. MacEwan, K.M. Dublin, K.R. Mann, An electronic nose transducer array of vapoluminescent platinum(II) double salts, J. Am. Chem. Soc. 123 (2001) 8414–8415;
(b) S.M. Drew, D.E. Janzen, K.R. Mann, Characterization of a cross-reactive electronic nose with vapoluminescent array elements, Anal. Chem. 74 (2002) 2547–2555;
(c) S.M. Drew, J.E. Mann, B.J. Marquardt, K.R. Mann, A humidity sensor based on vapoluminescent platinum(II) double salt materials, Sens. Actuators B 97 (2004) 307–312.
[9] I. Ugi, R. Meyr, o-Tolyl isocyanide, Org. Synth. 41 (1961) 101–104.
[10] O.F. Wendt, N.F.K. Kaiser, L.I. Elding, Acetonitrile and propionitrile exchange at palladium(II) and platinum(II), J. Chem. Soc., Dalton Trans. (1997) 4733–4738.
[11] V.Y. Kukushkin, A. Oskarsson, L.I. Elding, Tetrakis(propanenitrile)platinum(II) trifluoromethanesulfonate as a suitable intermediate in synthetic Pt(II) chemistry, Inorg. Synth. 31 (1997) 279–284.
[12] W.R. Mason, H.B. Gray, Electronic structures of square-planar complexes, J. Am. Chem. Soc. 90 (1968) 5721–5729.
[13] S. Ohe, Vapor Pressure Data—Antoine Parameters, www.s-ohe.com/Butanol_cal.html.
[14] J.E. Jackson, A User's Guide to Principal Components, John Wiley and Sons, New York, 1991.
[15] K.R. Beebe, R.J. Pell, M.B. Seasholtz, Chemometrics: A Practical Guide, John Wiley and Sons, New York, 1998.
[16] (a) S.M. Drew, L.I. Smith, K.A. McGee, K.R. Mann, A platinum(II) extended linear chain material that selectively uptakes benzene, Chem. Mater. 21 (2009) 3117–3124;
(b) A.G. Dylla, D.E. Janzen, M.K. Pomije, K.R. Mann, A comparison of isomers: trans- and cis-dicyanobis(para-ethylisocyanobenzene)platinum, Organometallics 26 (2007) 6243–6247;
(c) C.E. Buss, K.R. Mann, Synthesis and characterization of $Pt(CN\text{-}p\text{-}(C_2H_5)C_6H_4)_2(CN)_2$, a crystalline vapoluminescent compound that detects vapor-phase aromatic hydrocarbons, J. Am. Chem. Soc. 124 (2002) 1031–1039.

Biographies

Matthew J. Cich was an undergraduate at Carleton College and is currently a graduate student at SUNY Stony Brook.

Ian M. Hill was an undergraduate at Carleton College and is currently a graduate student at the University of Minnesota.

Aaron D. Lackner was an undergraduate at Carleton College and is currently a graduate student at the University of California, Berkeley.

Ryan J. Martinez was an undergraduate at Carleton College and is currently a research assistant at the University of Minnesota.

Travis C. Ruthenburg was an undergraduate at Carleton College and is currently a graduate student at the University of California, Davis.

Yuichiro Takeshita was an undergraduate at Carleton College and is currently a graduate student at the Scripts Oceanographic Institute.

Andrew J. Young was an undergraduate at Carleton College and is currently a graduate student at the University of Illinois, Urbana-Champaign.

Steven M. Drew is a Professor of Chemistry at Carleton College. He received his Ph.D. at the University of Colorado and completed a post doctoral appointment at the University of North Carolina, Chapel Hill before joining the faculty at Carleton in 1991.

Carrie E. Buss received her Ph.D. from the University of Minnesota and is currently a staff scientist at Seagate in Bloomington, Minnesota.

Kent R. Mann is a Distinguished Teaching Professor and Merck Professor of Inorganic and Materials Chemistry at the University of Minnesota. He received his Ph.D. under the direction of Harry Gray at the California Institute of Technology.